

Advanced turning maneuver of a many-legged robot using pitchfork bifurcation

Shinya Aoi¹, Ryoe Tomatsu¹, Yuki Yabuuchi¹, Daiki Morozumi¹, Kota Okamoto¹, Soichiro Fujiki², Kei Senda¹, and Kazuo Tsuchiya¹

¹ Dept. of Aeronautics and Astronautics, Graduate School of Engineering, Kyoto University, Kyoto daigaku-Katsura, Nishikyo-ku, Kyoto 615-8540, Japan

² Dept. of Physiology and Biological Information, School of Medicine, Dokkyo Medical University, 880 Kita-Kobayashi, Mibu-machi, Shimotsuga-gun Tochigi 321-0293, Japan

Abstract—Legged robots have excellent terrestrial mobility for traversing diverse environments and thus have the potential to be deployed in a wide variety of scenarios. However, they are susceptible to falling and leg malfunction during locomotion. Although the use of a large number of legs can overcome these problems, it makes the body long and leads to many contact legs being constrained on the ground to support the long body, which impedes maneuverability. To improve the locomotion maneuverability of the robots, the present study focuses on dynamic instability, which induces rapid and large movement changes, and uses a 12-legged robot with flexible body axis. Our previous work found that the straight walk of the robot becomes unstable through Hopf bifurcation when the body axis flexibility is changed, which induces body undulations. Furthermore, we developed a simple controller based on the Hopf bifurcation and showed that the straight walk instability facilitates the turning of the robot. In this study, we newly found that the straight walk becomes unstable through pitchfork bifurcation when the body-axis flexibility is changed in a different way from that in our previous work. The pitchfork bifurcation not only induces the straight walk instability but also the transition into the curved walk, whose curvature can be controlled by the body-axis flexibility. We developed a simple controller based on the pitchfork-bifurcation characteristics and demonstrated that the robot can perform a turning maneuver superior to the previous controller based on the Hopf bifurcation. This study provides a novel design principle for maneuverable locomotion of many-legged robots using intrinsic dynamic properties.

Index Terms—Many-legged robot, Maneuverability, Instability, Pitchfork bifurcation, Curved walk, Turning

I. INTRODUCTION

Legged locomotion, such as that of animals, allows excellent terrestrial mobility for traversing diverse environments. Legged robots thus have potential to be deployed in a wide variety of scenarios, such as search and rescue [18], [29], hazardous environment operation and exploration [8], [42], and planetary exploration [5], [46]. Various legged robots with agile animal-like locomotion have recently been developed [1], [4], [19]–[21], [25], [27], [30], [31], [34], [38]. However, most of these robots have four legs and falling, which may result in the breakdown of mechanical and electrical components and from which it is difficult to recover, is inevitable during locomotion. Furthermore, damage to even one leg greatly degrades their locomotive performance [11]. The use of a large

number of legs prevents falling and allows a certain level of leg malfunction to be tolerated [22], [28].

Although the use of a large number of legs has advantages for legged robots, it makes the body long and motion planning and control difficult due to the many intrinsic degrees of freedom and complex interaction with the environment. In particular, many contact legs are physically constrained on the ground to support the long body, which can impede maneuverability. The underlying mechanism of agile locomotion using a large number of legs remains unclear from biological and engineering viewpoints [16]. Maneuverable locomotion for robots with a large number of legs remains challenging.

Conventional controllers precisely plan the motion of all degrees of freedom of the robot (e.g., how the long body is bent, where each foot touches the ground, and in what order the legs move) and control the robot to stabilize the desired motion. However, this approach has huge computational and energy costs, making it inefficient. To design a simple and efficient controller with high locomotor performance, the fundamental dynamic principles embedded in the robot dynamics including the interaction with the environment should be fully utilized [1], [9], [24], [25].

For maneuverable locomotion of many-legged robots that overcomes the above difficulties and the limitations of conventional approaches, the present study focuses on dynamic instability, which induces rapid and large movement changes, and uses a 12-legged robot whose body axis is flexible. Our previous work [2] showed that although many contact legs can impede maneuverability, they induce straight walk instability and body undulations through Hopf bifurcation when the body-axis flexibility is changed. Stability refers to the capability to resist and recover from disturbances; straight walk instability is thus expected to allow the robot to easily change walking direction. Therefore, we developed a simple controller based on the straight walk instability induced by the Hopf bifurcation to change walking direction without precise motion planning and control, and demonstrated that the straight walk instability facilitates the turning of the robot [3].

In the present study, we show that the pitchfork bifurcation of the straight walk is caused by changes in the body-axis flexibility in a different way from that in previous work [2], [3]. The pitchfork bifurcation not only destabilizes straight

walking, but also causes curved walking, where the flexible body axis forms a curved shape. Furthermore, we found that the curvature of curved walking can be controlled by the body-axis flexibility. We developed a simple control strategy based on the pitchfork-bifurcation characteristics, which improved the turning maneuver compared to that achieved using Hopf bifurcation. This study provides a design principle for a simple and efficient control scheme to create maneuverable locomotion for many-legged robots using intrinsic dynamic properties.

II. ROBOT

We used the many-legged robot developed in [2] and improved in [3]. The total length and mass are 135 cm and 8.5 kg, respectively. The robot consists of 6 body segment modules (modules 1–6), as shown in Fig. 1. Each module is composed of a single body and one pair of legs and has the same length. The body segments are passively connected by yaw joints (yaw joints 1–5) onto which torsional springs and potentiometers are installed. The yaw joint angles are zero when the body segments were aligned. Each leg has two links connected by pitch joints. The legs in the first module (module 1) have an additional link connected by a yaw joint to supplement the control of the walking direction during turning tasks. Each leg joint is manipulated by an encoder-equipped motor. The first module has a laser range scanner (Hokuyo, URG-04LX) to find the relative position of a target for turning. The robot was controlled by an external host computer (Intel Pentium 4 2.8 GHz, RT-Linux) with 2-ms intervals, and walked on a wooden flat floor with a vinyl floor mat to suppress slipping. The computer control signals and electric power were provided via external cables, which were kept slack and suspended to avoid influencing the locomotor behavior of the robot.

To make the robots walk in a straight line, we controlled the legs using the two pitch joints of each leg to follow the desired movement, which consists of two parts, namely half of an elliptical curve that starts from the posterior extreme position (PEP) and ends at the anterior extreme position (AEP), and a straight line from the AEP to the PEP (Fig. 1B). In the straight line, the leg tips moved from the AEP to the PEP at a constant speed parallel to the body. We set the duration of the half elliptical curve to 0.29 s, that of the straight line to 0.31 s, and the distance between the AEP and the PEP in each leg to 3 cm. The left and right legs in each module moved in antiphase, and the relative phase between the ipsilateral legs on adjacent modules was set to $2\pi/3$ rad. When the leg yaw joint angles of the first module were fixed so that the leg tip trajectories were parallel to the body, the robot was expected to walk in a straight line while keeping the body segments parallel to each other because torsional springs were installed on the body-segment yaw joints and all support-leg tips moved parallel to the body segments at an identical speed.

III. PITCHFORK BIFURCATION OF STRAIGHT WALK

A. Experimental results

Our previous work [2], [3] revealed that when we used torsional springs with the same spring constant for all body-segment yaw joints (yaw joints 1–5) and changed the spring

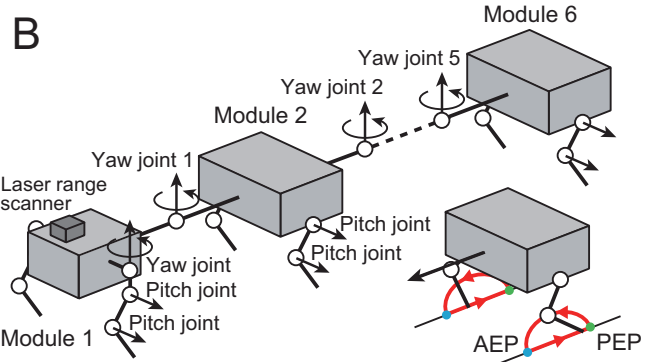
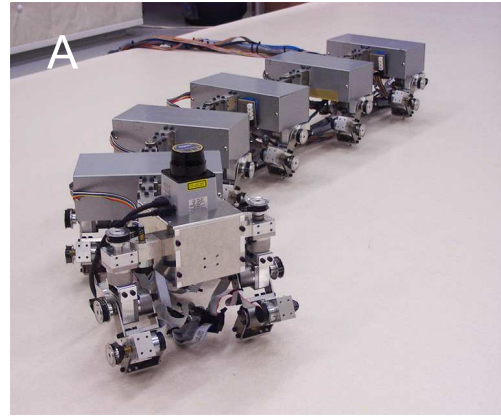


Fig. 1. (A) Photograph and (B) schematic model of many-legged robot. The robot consists of 6 modules, each of which has one body segment and one pair of legs. The legs are controlled by two pitch joints so that the leg tips follow a periodic trajectory, including the anterior extreme position (AEP) and the posterior extreme position (PEP). Body segments are passively connected by yaw joints with installed torsional springs. The legs in the first module have additional yaw joints to change walking direction. The laser range scanner is installed on the first module to find a position relative to a target.

constant uniformly among the joints, the straight walk became unstable through Hopf bifurcation, which induced body undulations. This bifurcation was verified by a Floquet analysis with a simple physical model. In this study, we performed robot experiments of walking in a straight line, where we changed the body axis flexibility in a way that was different from that in our previous work. Specifically, we used the same spring constant for yaw joints 2–5 ($k_i = 41$ Nmm/deg, $i = 2, \dots, 5$) and used various spring constants for yaw joint 1 ($k_1 = 15, 17, 21, 28, 41,$ and 75 Nmm/deg). We set all the body segments parallel to each other as the initial conditions. The leg yaw joints in the first module were fixed during the experiments.

When we used large spring constants for k_1 , the robot kept walking in a straight line as expected, and the body segments were aligned, with all body-segment yaw joint angles being almost zero (Figs. 2A and E, see Movie 1). However, when k_1 was set to below a threshold value, the body-segment yaw joints showed non-zero angles with the same sign; that is, the body axis was curved and the robot walked in a curved line (Figs. 2B, F, and G, see Movies 2 and 3). Specifically, the robot walked in a curved line for $k_1 = 15, 17, 21,$ and 28 Nmm/deg, but not for $k_1 = 41$ and 75 Nmm/deg.

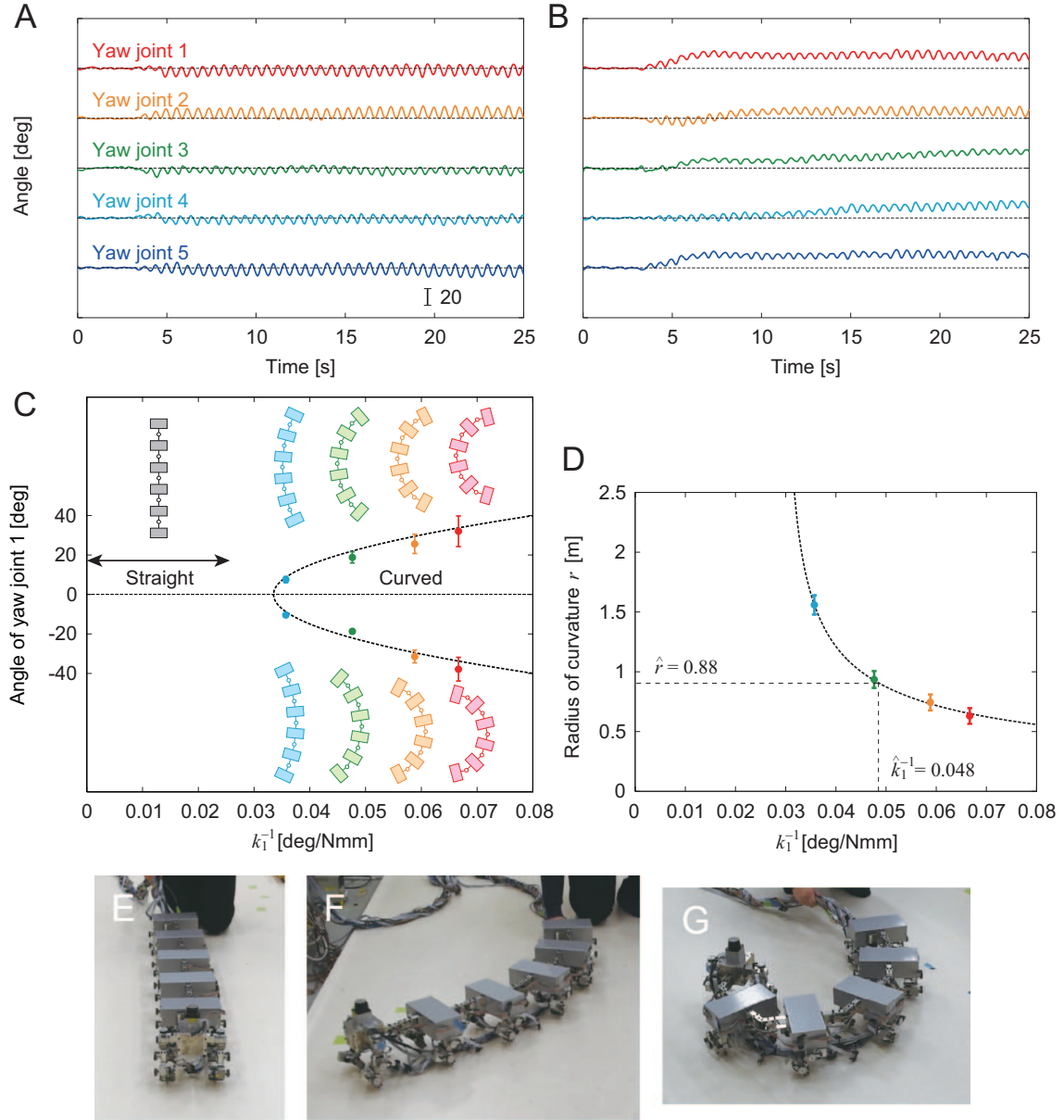


Fig. 2. Characteristics of curved walk for k_1 values below threshold value. Yaw joint angles for (A) straight walk with $k_1 = 41$ Nmm/deg and (B) curved walk with $k_1 = 15$ Nmm/deg (see Movies 1–3). (C) Average angle of yaw joint 1 during curved walk for $1/k_1$ that indicates pitchfork bifurcation. The data points and error bars correspond to the means and standard errors, respectively, of the results of five experiments. (D) Radius of curvature of body axis for $1/k_1$. The data points and error bars correspond to the means and standard errors, respectively, of the results of ten experiments. Photographs for (E) straight walk with $k_1 > \hat{k}_1$, (F) curved walk with small curvature with $k_1 \sim \hat{k}_1$, and (G) curved walk with large curvature with $k_1 < \hat{k}_1$.

Furthermore, both left- and right-curved walking could be achieved depending on the initial robot conditions. Figure 2C shows the angles of yaw joint 1 for $1/k_1$ averaged over 5 s during a curved walk (the angles for the other body-segment yaw joints are shown in Fig. 3). The magnitude of these angles increases with $1/k_1$. These results suggest that the presence of pitchfork bifurcation depends on k_1 . These angle data were fitted by the square root of $1/k_1$ [39]. The bifurcation point was estimated to be $k_1 = 34$ Nmm/deg ($1/k_1 = 0.030$ deg/Nmm).

The dependence of the body-segment yaw joint angles on $1/k_1$ (Fig. 2C and Fig. 3) indicates the change of the curved

shape of the body axis for the curved walk. Figure 2D shows the radius of curvature r of the body axis for $1/k_1$ calculated as $r = 5L / \sum_{i=1}^5 |\theta_i|$, where θ_i is the angle of yaw joint i ($i = 1, \dots, 5$) and L is the length of the body segments. This figure shows that we can control the curvature of the body axis to perform a curved walk by adjusting k_1 through pitchfork bifurcation.

B. Verification by Floquet analysis with simple physical model

The robot experiments suggested that the presence of pitchfork bifurcation in the straight walk depends on the spring constant k_1 (Figs. 2C and 3). We verified this bifurcation

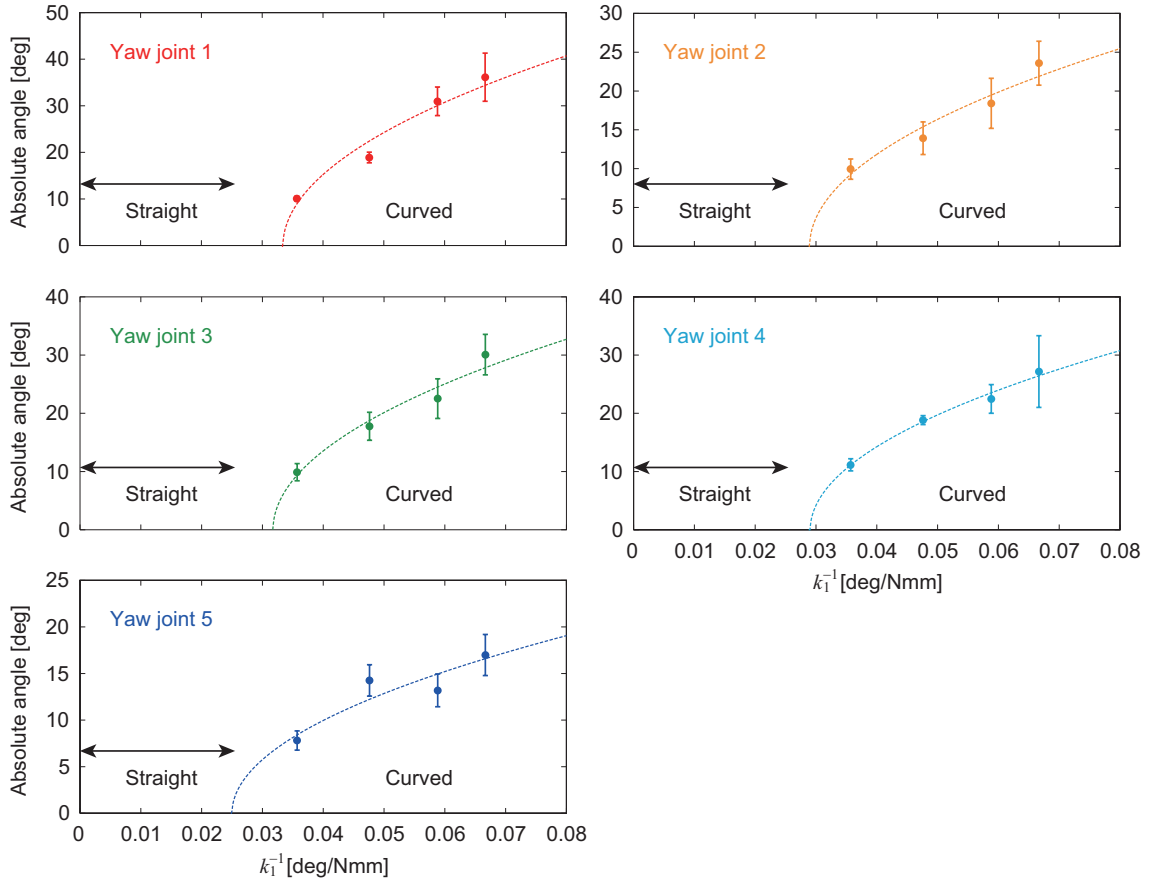


Fig. 3. Average absolute angles of body-segment yaw joints during curved walk for $1/k_1$. The data points and error bars correspond to the means and standard errors, respectively, of the results of ten experiments.

from a theoretical viewpoint using a Floquet analysis with a simple physical model, as done in our previous work [2]. The model was simplified from the original high-dimensional mechanical model to extract the fundamentals of locomotion dynamics (Fig. 4A). In particular, the model was two-dimensional because the movements were designed to make the robots walk without up-and-down, roll, or pitch motions of the body segments. Furthermore, because an important role of legs in locomotion is to receive reaction forces from the floor, we neglected the inertial force of the legs and used the geometric constraint forces of the leg tips. The equations of motion were linearized around the state of a straight walk, and the Floquet exponents were investigated on the complex plane. In previous work, when all the spring constants for the body-segment yaw joints were decreased uniformly, one pair of exponents crossed the imaginary axis from the left-half plane and entered the right-half plane, which implied Hopf bifurcation. Figure 4B shows all 16 Floquet exponents when k_1 was varied, with the other spring constants k_i ($i = 2, \dots, 5$) fixed, as done in the robot experiments. Except for the zero exponents, all exponents lie in the left-half plane for large k_1 . However, with decreasing k_1 , one exponent moves along the real axis and enters the right-half plane. This indicates that the straight walk becomes unstable and pitchfork bifurcation occurs above a critical value of k_1 . Furthermore, the

components of the destabilizing eigenvector at the bifurcation point were 0.31, 0.16, 0.21, 0.21, and 0.11 for yaw joints 1–5, respectively. These components had the same sign, and yaw joints 1 and 5 had large and small components, respectively, which is consistent with the robot experiments (Fig. 3). These results verify the destabilization of the straight walk and the emergence of a curved walk through pitchfork bifurcation observed in the robot experiments.

IV. TURNING MANEUVERABILITY

A. Turning strategy based on pitchfork bifurcation

To investigate the maneuverability of the robots achieved with the aid of pitchfork bifurcation, we focused on a turning task in which the robot approached a target located on the floor in a direction different from that where the robot was oriented, as performed in our previous work [3]. For a target at any location (relative angle ψ and distance R), there exists a unique radius of curvature \hat{r} of the curved walk with which the robot will approach the target (Fig. 5A). Because the radius of curvature r of the body axis induced by the pitchfork bifurcation monotonically decreases with $1/k_1$ (Fig. 2D), $k_1 = \hat{k}_1$ is uniquely determined so that $r = \hat{r}$. This means that when we use $k_1 = \hat{k}_1$, the robot spontaneously approaches the target due to the pitchfork bifurcation characteristics, which is an optimal strategy for turning. However, this strategy is

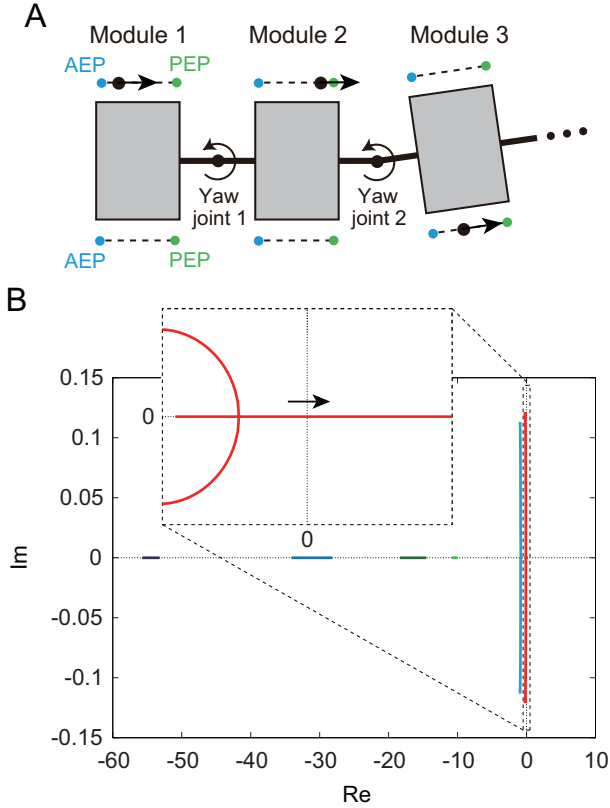


Fig. 4. Floquet analysis using simple two-dimensional model. (A) simple model. (B) Floquet exponents when k_1 was varied.

feedforward, depending only on the initial relative position between the robot and the target, and the direction in which the robot turns (left or right) depends on the initial robot conditions, and thus does not guarantee the success of the turning tasks. Therefore, we also used a supplementary turning controller to approach the target by means of the laser range scanner and leg yaw joints of the first module developed in our previous work [3] (see Appendix B). This supplementary controller allowed the robots to approach the targets even when $k_1 \neq \hat{k}_1$.

B. Experimental results

For the initial conditions, we used $\psi = 45^\circ$ and $R = 1.3$ m for the relative angle and distance between the first module and the target, respectively, which yielded $\hat{r} = 0.88$ m and $\hat{k}_1 = 21$ Nmm/deg ($1/\hat{k}_1 = 0.048$ deg/Nmm), and set all body-segment yaw joint angles to zero (Fig. 5F). Figure 5B shows the trajectory of the first module on the floor during the turning task for three torsional spring constants, namely $k_1 = 15$ ($< \hat{k}_1$), 21 ($\sim \hat{k}_1$), and 41 Nmm/deg ($> \hat{k}_1$). Figures 5C and D show the time profiles of the target distance and relative target angle with respect to the walking direction, respectively, for these three spring constants. When the distance was less than 0.15 m, we assumed that the robot reached the target and this task was successfully completed. For $k_1 = 41$ Nmm/deg ($> \hat{k}_1$), the robot hardly changed walking direction and the first module trajectory bulged outward. As a result, the

robot could not reach the target (Fig. 5G, see Movie 4). For $k_1 = 15$ Nmm/deg ($< \hat{k}_1$), although the robot could quickly change walking direction, it moved in directions away from the target due to the small radius of curvature created by pitchfork bifurcation and could not reach the target (Fig. 5I, see Movie 5). In contrast, for $k_1 = 21$ Nmm/deg ($\sim \hat{k}_1$), the robot reached the target through the optimal curved walk generated by pitchfork bifurcation (Fig. 5H, see Movie 6).

To quantitatively clarify the turning performance dependence on k_1 , we employed two evaluation criteria, namely ε_1 and ε_2 . For the criterion ε_1 , we used the distance of the target at 23 s to evaluate how quickly and successfully the robot approached the target. For the criterion ε_2 , we used the absolute value of the relative target angle with respect to the walking direction to evaluate how quickly and successfully the robot was oriented to the target. Figure 5E shows the results for $1/k_1$. Both criteria showed minimum values around $k_1 = \hat{k}_1$, which means that the turning strategy using pitchfork bifurcation achieved the best performance and that the robot made the best use of the curved walk induced by pitchfork bifurcation to complete the turning task.

To verify the performance of the proposed controller using pitchfork bifurcation, we additionally performed the same experiment as that in Fig. 5B but using different initial conditions of the target, namely $\psi = 40^\circ$ and $R = 1.5$ m, which yielded $\hat{r} = 1.2$ m and $\hat{k}_1 = 26$ Nmm/deg ($1/\hat{k}_1 = 0.039$ deg/Nmm). Figures 6A and B show the evaluation criteria ε_1 and ε_2 , respectively, for $1/k_1$. Both criteria show minimum values around $k_1 = \hat{k}_1$, which means that the turning strategy using pitchfork bifurcation achieved the best performance, in the same way as shown in Fig. 5E. The results show similar trends, which verifies the performance of the proposed controller.

C. Comparison with previous strategy

To examine how the turning performance was improved by pitchfork bifurcation, we also performed experiments using the turning strategy based on Hopf bifurcation used in our previous work [3] and compared the performance. For Hopf bifurcation, we used the same spring constant among the body-segment yaw joints and employed five spring constants ($k_i = 8.7, 11, 15, 21, \text{ and } 41$ Nmm/deg, $i = 1, \dots, 5$) to evaluate the turning performance for k_i , where the Hopf bifurcation point is about $k_i = 18$ Nmm/deg ($1/\hat{k}_i = 0.057$ deg/Nmm), as obtained in our previous work [3]. The experimental conditions were identical to those in Fig. 5E except for the spring constants of the body-segment yaw joints. Figures 7A and B compare the turning performance in terms of the criteria ε_1 and ε_2 , respectively, between the strategies based on pitchfork and Hopf bifurcations. Both criteria for Hopf bifurcation showed minimum values in the unstable region, as observed in our previous work [3]. The minimum values of pitchfork bifurcation are lower than those of Hopf bifurcation for both criteria. This means that the turning strategy based on pitchfork bifurcation created by tuning the body-axis flexibility is superior to that based on Hopf bifurcation.

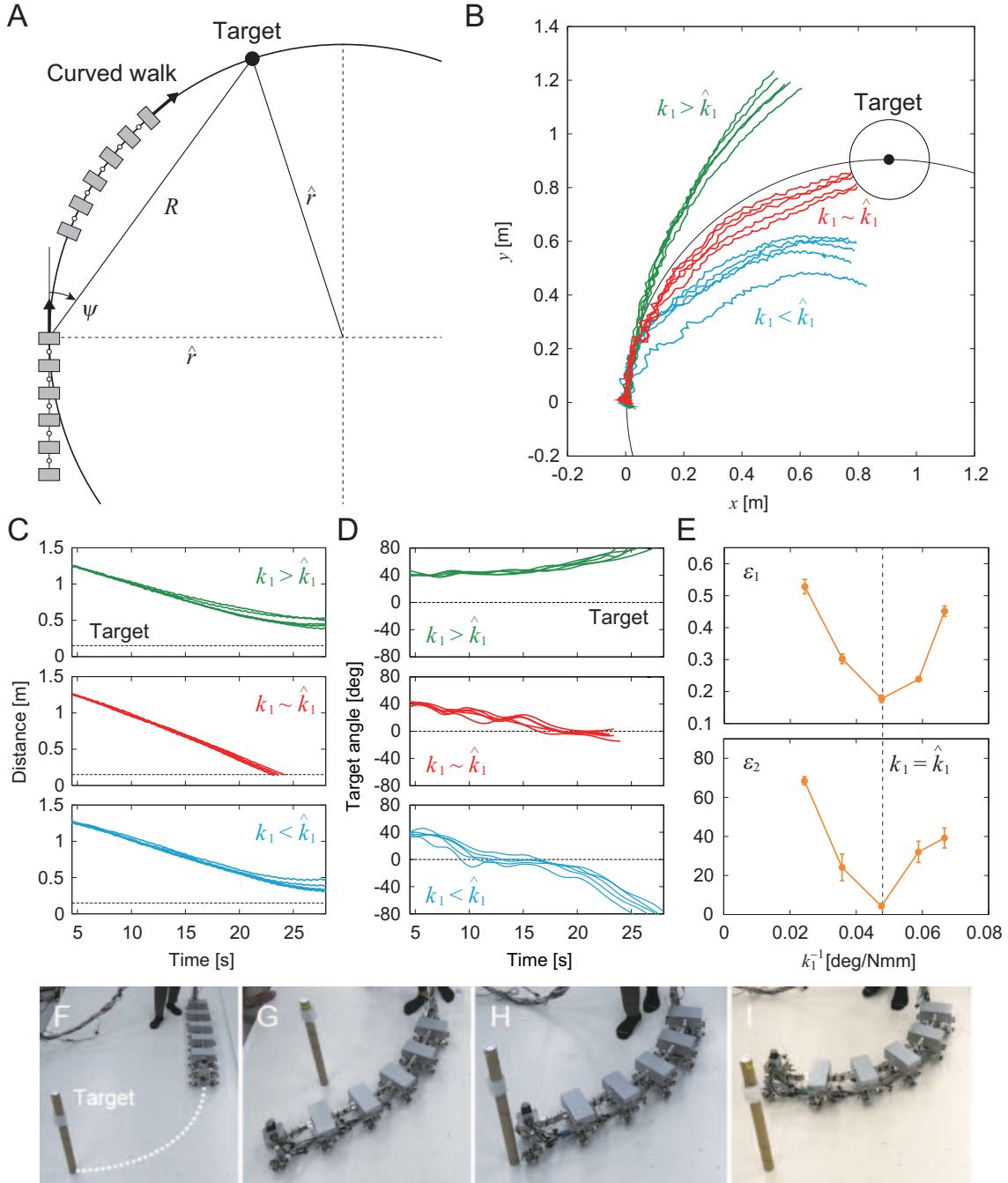


Fig. 5. Turning task. (A) Radius of curvature \hat{r} of curved walk with which the robot approaches a target (relative angle ψ and distance R). (B) Trajectory of the first module on the floor, (C) target distance, and (D) relative target angle for five experiments for three spring constants with $\psi = 45^\circ$, $R = 1.3$ m, $\hat{r} = 0.88$ m, and $1/\hat{k}_1 = 0.048$ deg/Nmm (see Movies 4–6). (E) Evaluation criteria ε_1 and ε_2 for $1/k_1$. The data points and error bars correspond to the means and standard errors, respectively, of the results of five experiments. Photographs for (F) initial conditions, (G) unsuccessful approach with $k_1 > \hat{k}_1$, (H) successful approach with $k_1 \sim \hat{k}_1$, and (I) unsuccessful approach with $k_1 < \hat{k}_1$.

V. CONCLUSION AND DISCUSSION

In this study, we found that the straight walk of a many-legged robot with flexible body axis becomes unstable through pitchfork bifurcation when the body-axis flexibility is changed. The straight walk transitioned into curved walk, whose curvature depended on the body-axis flexibility. We developed a simple controller based on the pitchfork-bifurcation characteristics and demonstrated that the robot achieves high turning maneuver superior to the previous controller based on the Hopf bifurcation.

Maneuverability is related to the ability to change movement direction. When the movement direction is destabilized during locomotion, the instability provides driving forces to rapidly change the movement direction and thus enhances maneuverability. Some fighter aircrafts, such as the F-16, are designed to be aerodynamically unstable to enhance maneuverability [7], [23]. The use of dynamic instability is thus useful from an engineering viewpoint.

The strategy of using movement direction instability to enhance maneuverability is also used by animals. Because

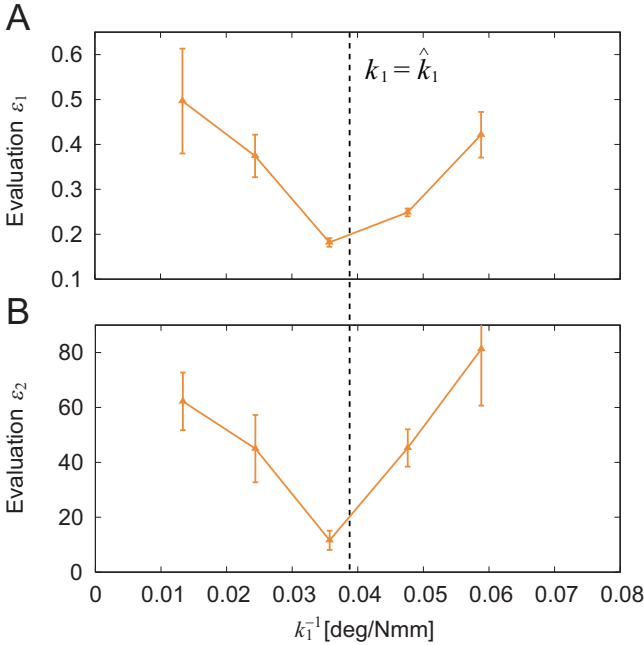


Fig. 6. Evaluation criteria (A) ε_1 and (B) ε_2 for $1/k_1$ for different condition ($1/\hat{k}_1 = 0.039$ deg/Nmm). The data points and error bars correspond to the means and standard errors, respectively, of the results of five experiments.

the instability is determined by the body dynamics during interaction with the environment, it is prominent in locomotion generated through aerodynamics and hydrodynamics, such as the locomotion of flying insects [13], [32], [41] and sea animals [14], [15], [44]. It also appears in legged locomotion. When the center of mass is high, as in mammals, whose legs are under the body, leaning the body to the left or right induces instability and helps turning [10], [35]. However, when the center of mass is low, as in reptiles and arthropods, whose legs are out to the side of the body, locomotor behavior is almost two-dimensional because the center of mass moves in a horizontal plane. Therefore, the effect of body leaning is small and thus such a turning strategy cannot be used, which implies that the stability of the walking direction in the horizontal plane becomes more crucial. It has been suggested that cockroaches manipulate the position of the reaction forces from the floor entering the body to control the stability of a straight walk in a horizontal plane and that the straight walk instability helps their turning [33], [35].

Various bio-inspired robots that use their body axis for propulsion, such as snake robots [6], [37] and fish robots [12], [26], [36], have high maneuverability. However, legged robots still have difficulty in achieving highly maneuverable locomotion. This is partly because their interaction with the environment (i.e., foot contact with the ground) is intermittent due to the repetition of foot-contact and foot-off phases in leg movement. Although this intermittency allows the traversal of diverse environments, it can make the robot lose balance. Therefore, the control design of legged robots has focused on the avoidance of balance loss using dynamic criteria, such as a supporting polygon [17] and a zero-moment point [43], and maneuverability has not been well investigated. Although

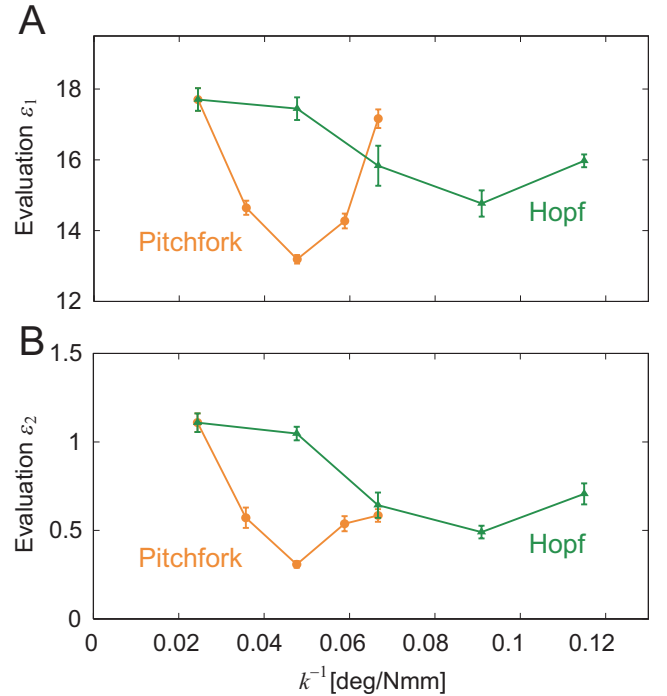


Fig. 7. Comparison of evaluation criteria (A) ε_1 and (B) ε_2 between the turning strategies based on pitchfork bifurcation and Hopf bifurcation. The data points and error bars correspond to the means and standard errors, respectively, of the results of five experiments.

increasing the number of legs prevents balance loss, it also increases the number of contact legs, which impedes maneuverability. Moreover, the number of degrees of freedom to be controlled increases, making both motion planning and control difficult. In addition, general many-legged robots use actuators for controlling not only the leg joints but also body-segment joints [40], [45], which has huge computational and energy costs. In contrast, our robot has passive body-segment joints and turning controller is simple, which does not directly control the movement of the body axis and instead determines the body-axis flexibility based on the pitchfork bifurcation characteristics inherent in the robot dynamics. The generation of robot movements not by actuators but by dynamics is crucial for efficient locomotion [9], and our strategy greatly reduces the computational and energy costs. This study provides a design principle for a simple and efficient control scheme to create maneuverable locomotion for many-legged robots using intrinsic dynamic properties. The proposed turning strategy can be further improved. For example, variable stiffness can be used for the body-segment yaw joints to change the stability characteristics depending on the task and conditions.

APPENDIX A SUPPLEMENTARY MOVIES

We recorded 6 supplementary movies to show the pitchfork bifurcation of a straight walk and turning performance in the robot experiments:

Movie 1: Straight walk using a large spring constant for the torsional spring in yaw joint 1.

- Movie 2: Curved walk with a small curvature using a small spring constant for the torsional spring in yaw joint 1.
- Movie 3: Curved walk with a large curvature using very small spring constant for the torsional spring in yaw joint 1.
- Movie 4: Unsuccessful approach using a spring constant larger than the optimal value for yaw joint 1.
- Movie 5: Unsuccessful approach using a spring constant smaller than the optimal value for yaw joint 1.
- Movie 6: Successful approach using a spring constant close to the optimal value.

APPENDIX B

SUPPLEMENTARY TURNING CONTROL BY LEG JOINTS

The optimal turning strategy is feedforward, depending only on the initial relative position between the robot and target. In addition, the direction in which the robot turns (left or right) depends on the initial robot conditions because of the property of pitchfork bifurcation. To guarantee a successful approach to the target, we used a supplementary feedback-based turning controller, which was developed in our previous work [3]. Specifically, we used the relative target angle ψ of the first module measured by the laser range scanner and the leg yaw joints θ_1 and θ_2 of the first module. We determined the desired angles $\hat{\theta}_1$ and $\hat{\theta}_2$ of θ_1 and θ_2 for each gait cycle ($t_i^n \leq t < t_i^n + T$, $t = t_i^n$ is the time when the desired leg tip is at the PEP for the n th gait cycle, and T is the gait cycle duration (= 0.6 s)) using

$$\hat{\theta}_i(t) = \begin{cases} \hat{\theta}_i(t_i^n) & t_i^n \leq t < t_i^n + t_{\text{start}} \\ \hat{\theta}_i(t_i^n) + \Delta_i \frac{t - t_i^n - t_{\text{start}}}{t_{\text{end}} - t_{\text{start}}} & t_i^n + t_{\text{start}} \leq t \leq t_i^n + t_{\text{end}} \\ \hat{\theta}_i(t_i^n + t_{\text{end}}) & t_i^n + t_{\text{end}} < t < t_i^n + T \end{cases}$$

$$\Delta_i = \begin{cases} \psi(t_i^n + t_{\text{start}}) - \hat{\theta}_i(t_i^n + t_{\text{start}}) & |\psi(t_i^n + t_{\text{start}}) - \hat{\theta}_i(t_i^n + t_{\text{start}})| < 5^\circ \\ 5^\circ & \text{otherwise} \end{cases}$$

where t_{start} and t_{end} were set to 40% and 80%, respectively, of the duration of the half elliptical curve of the leg tip trajectory (= 0.12 and 0.23 s). This means that each leg changed its yaw direction toward the target only during the swing phase with 5° of the maximum turning angle for one gait cycle. We also limited the maximum angle of the leg yaw joint to 5° during the turning task. This supplementary control did not aim to make the robots follow the optimal curved path generated by the turning strategy using pitchfork bifurcation. Instead, it was designed so that the first module modulated the walking direction based on the target direction, which solves the problems related to the feedforward property of the optimal turning strategies and the turning direction due to initial robot conditions, and furthermore allows the robots to approach the target even when $k_1 \neq \hat{k}_1$.

ACKNOWLEDGMENT

This study was supported in part by JSPS KAKENHI Grant Numbers JP17H04914 and JP19KK0377 and the Inamori Foundation.

REFERENCES

- [1] Aguilar, J., Zhang, T., Qian, F., Kingsbury, M., McInroe, B., Mazouchova, N., Li, C., Maladen, R., Gong, C., Travers, M., Hatton, R.L., Choset, H., Umbanhowar, P.B. & Goldman, D.I. A review on locomotion robophysics: the study of movement at the intersection of robotics, soft matter and dynamical systems. *Rep. Prog. Phys.* **79**, 110001 (2016).
- [2] Aoi, S., Egi, Y. & Tsuchiya, K. Instability-based mechanism for body undulations in centipede locomotion. *Phys. Rev. E* **87**, 012717 (2013).
- [3] Aoi, S., Tanaka, T., Fujiki, S., Funato, T., Senda, K. & Tsuchiya, K. Advantage of straight walk instability in turning maneuver of multilegged locomotion: a robotics approach. *Sci. Rep.* **6**, 30199 (2016).
- [4] Aoi, S., Manoonpong, P., Ambe, Y., Matsuno, M. & Wörgötter, F. Adaptive control strategies for interlimb coordination in legged robots: A review. *Front. Neurobot.* **11**, 39 (2017).
- [5] Arm, P., Zenkl, R., Barton, P., Beglinger, L., Dietsche, A., Ferrazzini, L., Hampp, E., Hinder, J., Huber, C., Schaufelberger, D., Schmitt, F., Sun, B., Stolz, B., Kolvenbach, H. & Hutter, M. SpaceBok: A dynamic legged robot for space exploration, In *Proc. IEEE Int. Conf. Robot. Autom.*, pp. 6288-6294 (2019).
- [6] Astley, H.C., Gong, C., Daib, J., Travers, M., Serrano, M.M., Vela, P.A., Choset, H., Mendelson III, J.R., Hu, D.L., and Goldman, D.I. Modulation of orthogonal body waves enables high maneuverability in sidewinding locomotion. *Proc. Natl. Acad. Sci. USA* **112**, 6200-6205 (2015).
- [7] Avanzini, G. & de Matteis, G. Bifurcation analysis of a highly augmented aircraft model. *J. Guid. Contr. Dyn.* **20**, 754-759 (1997).
- [8] Byrd, J.S. & DeVries, K.R. A six-legged telerobot for nuclear applications development. *Int. J. Robot. Res.* **9**, 43-52 (1990).
- [9] Collins, S.H., Ruina, A.L., Tedrake, R. & Wisse, M. Efficient bipedal robots based on passive-dynamic walkers. *Science* **307**, 1082-1085 (2005).
- [10] Courtine, G. & Schieppati, M. Human walking along a curved path. II. Gait features and EMG patterns. *Eur. J. Neurosci.* **18**, 191-205 (2003).
- [11] Cully, A., Clune, J., Tarapore, D. & Mouret, J.-B. Robots that can adapt like animals. *Nature* **521**, 503-507 (2015).
- [12] Curet, O.M., Patankar, N.A., Lauder, G.V. & MacIver, M.A. Aquatic manoeuvring with counter-propagating waves: A novel locomotive strategy. *J. R. Soc. Interface* **8**, 1041-1050 (2011).
- [13] Dickinson, M.H., Farley, C.T., Full, R.J., Koehl, M.A.R., Kram, R. & Lehman, S. How animals move: An integrative view. *Science* **288**, 100-106 (2000).
- [14] Fish, F.E., Hurley, J. & Costa, D.P. Maneuverability by the sea lion *Zalophus californianus*: turning performance of an unstable body design. *J. Exp. Biol.* **206**, 667-674 (2003).
- [15] Fish, F.E. Balancing requirements for stability and maneuverability in cetaceans. *Integr. Comp. Biol.* **42**, 85-93 (2002).
- [16] Full, R.J., Kubow, T., Schmitt, J., Holmes, P. & Koditschek, D. Quantifying dynamic stability and maneuverability in legged locomotion. *Integr. Comp. Biol.* **42**, 149-157 (2002).
- [17] Hirose, S. A study of design and control of a quadruped walking vehicle. *Int. J. Robot. Res.* **3**, 113-133 (1984).
- [18] Hoffman, K.L. & Wood, R.J. Myriapod-like ambulation of a segmented microbot. *Auton. Robot.* **31**, 103-114 (2011).
- [19] Hwangbo, J., Lee, J., Dosovitskiy, A., Bellicoso, D., Tsounis, V., Koltun, V. & Hutter, M. Learning agile and dynamic motor skills for legged robots. *Sci. Robot.* **4**, eaau5872 (2019).
- [20] Ijspeert, A.J., Crespi, A., Ryzcko, D. & Cabelguen, J.-M. From swimming to walking with a salamander robot driven by a spinal cord model. *Science* **315** 1416-1420 (2007).
- [21] Ijspeert, A.J. Biorobotics: Using robots to emulate and investigate agile locomotion. *Science* **346**, 196-203 (2014).
- [22] Kano, T., Sakai, K., Yasui, K., Owaki, D. & Ishiguro, A. Decentralized control mechanism underlying interlimb coordination of millipedes. *Bioinspir. Biomim.* **12**, 036007 (2017).
- [23] Kwatny, H.G., Bennett, W.H. & Berg, J. Regulation of relaxed static stability aircraft. *IEEE Trans. Automat. Contr.* **36**, 1315-1332 (1991).
- [24] Li, C., Umbanhowar, P.B., Komsuoglu, H., Koditschek, D.E. & Goldman, D.I. Sensitive dependence of the motion of a legged robot on granular media. *Proc. Natl. Acad. Sci. USA* **106**, 3029-3034 (2009).
- [25] Li, C., Zhang, T. & Goldman, D.I. A terradynamics of legged locomotion on granular media. *Science* **339**, 1408-1411 (2013).
- [26] Maladen, R.D., Ding, Y., Umbanhowar, P.B., Kamor, A. & Goldman, D.I. Mechanical models of sandfish locomotion reveal principles of high performance subsurface sand-swimming. *J. R. Soc. Interface* **8**, 1332-1345 (2011).

- [27] Mastalli, C., Havoutis, I., Focchi, M., Caldwell, D.G. & Semini, C. Motion planning for quadrupedal locomotion: Coupled planning, terrain mapping and whole-body control. *IEEE Trans. Robot.* **36**, 1635-1648 (2020).
- [28] Miguel-Blanco, A. & P. Manoonpong, General distributed neural control and sensory adaptation for self-organized locomotion and fast adaptation to damage of walking robots. *Front. Neural Circuits* **14**, 46 (2020).
- [29] Ning, M., Ma, Z., Chen, H., Cao, J., Zhu, C., Liu, Y. & Wang, Y. Design and analysis for a multifunctional rescue robot with four-bar wheel-legged structure. *Adv. Mech. Eng.* **10**, 1-14 (2018).
- [30] Owaki, D. & Ishiguro, A. A quadruped robot exhibiting spontaneous gait transitions from walking to trotting to galloping. *Sci. Rep.* **7**, 277 (2017).
- [31] Park, H-W., Wensing, P.M. & Kim, S. High-speed bounding with the MIT Cheetah 2: Control design and experiments. *Int. J. Robot. Res.* **36**, 167-192 (2017).
- [32] Parsons, M.M., Krapp, H.G. & Laughlin, S.B. Sensor fusion in identified visual interneurons. *Curr. Biol.* **20**, 624-628 (2010).
- [33] Proctor, J. & Holmes, P. Steering by transient destabilization in piecewise-holonomic models of legged locomotion. *Reg. Chaot. Dyn.* **13**, 267-282 (2008).
- [34] Raibert, M., Blankespoor, K., Nelson, G., Playter, R. & BigDog Team BigDog, the rough-terrain quadruped robot. In *Proc. IFAC World Congress*, pp. 10822-10825 (2008).
- [35] Schmitt, J. & Holmes, P. Mechanical models for insect locomotion: dynamics and stability in the horizontal plane - II. Application. *Biol. Cybern.* **83**, 517-527 (2000).
- [36] Sefati, S., Neveln, I.D., Roth, E., Mitchell, T.R.T., Snyder, J.B., MacIver, M.A., Fortune, E.S. & Cowan, N.J. Mutually opposing forces during locomotion can eliminate the tradeoff between maneuverability and stability. *Proc. Natl. Acad. Sci. USA* **110**, 18798-18803 (2013).
- [37] Stamper, S.A., Sefati, S. & Cowan, N.J. Snake robot uncovers secrets to sidewinders' maneuverability. *Proc. Natl. Acad. Sci. USA* **112**, 5870-5871 (2015).
- [38] Steingrube, S., Timme, M., Wörgötter, F. & Manoonpong, P. Self-organized adaptation of a simple neural circuit enables complex robot behaviour. *Nat. Phys.* **6**, 224-230 (2010).
- [39] Strogatz, S.H. *Nonlinear dynamics and chaos: With applications to physics, biology, chemistry, and engineering*, Perseus Books: New York (1994).
- [40] Takahashi, R. & Inagaki, S. Walk control of segmented multi-legged robot based on integrative control of legs and 2-DoF active intersegment joints. *Adv. Robot.* **30**, 1354-1364 (2016).
- [41] Taylor, G.K. & Krapp, H.G. Sensory systems and flight stability: What do insects measure and why? *Adv. Insect Physiol.* **34**, 231-316 (2007).
- [42] Toshiba corp. Quadruped robot for nuclear facilities, *E-J. Adv. Maint.* **6**, NT64 (2014).
- [43] Vukobratović, M., Borovac, B., Surla, D. & Stokić, D. *Biped locomotion-dynamics, stability, control and application*, Springer-Verlag (1990).
- [44] Webb, P.W. Designs for stability and maneuverability in aquatic vertebrates: What can we learn? In *Proc. Int. Symp. Unman. Unteth. Sub. Tech.*, pp. 86-108 (1997).
- [45] Wei, T., Luo, Q., Mo, Y., Wang, Y. & Cheng, Z. Design of the three-bus control system utilising periodic relay for a centipede-like robot. *Robotica* **34**, 1841-1854 (2016).
- [46] Wilcox, B.H., Litwin, T., Biesiadecki, J., Matthews, J., Heverly, M., Morrison, J., Townsend, J., Ahmad, N., Sirota, A. & Coope, B. Athlete: A cargo handling and manipulation robot for the moon. *J. Field Robot.* **24**, 421-434 (2007).